XL CILAMCE
IBERO-LATIN AMERICAN CONGRESS ON COMPUTATIONAL METHODS IN ENGINEERING
NOVEMBER 11-14, 2019
Praiamar Natal Hotel & Convention
Natal, RN-BRAZIL

OBTAINING PORE-SIZE DISTRIBUTION BY IMAGE ANALYSIS OF STACKS WITH LARGE IMAGE SPACING WITHOUT RESIZING

Adriano S. Rocha
Elizabeth M. B. D. Pontedeiro
Adriano.rocha@coc.ufrj.br
bettymay@petroleo.ufrj.br
Laboratory of Enhanced Oil Recovery (LRAP), Civil Engineering Program – COPPE/UFRJ
Rio de Janeiro/RJ, Brazil
José L. D. Alves
jalves@lamce.coppe.ufrj.br
Laboratory of Computational Methods in Engineering (LAMCE), Civil Engineering Program – COPPE/UFRJ
Rio de Janeiro/RJ, Brazil
W. G. A. L. Silva
wmgodoy@petroleo.ufrj.br
Laboratory of Enhanced Oil Recovery (LRAP), Civil Engineering Program – COPPE/UFRJ
Rio de Janeiro/RJ, Brazil

Abstract. The characterization of porous media is a crucial process to study the flow in porous structures and the pore-size distribution (PSD) is a fundamental parameter to perform this characterization. The PSD describes the porous volume fraction of each different pore-size. The PSD is usually estimated by laboratorial tests, which have long durations and may be sample destructive. Yang and collaborators developed an alternative capable to estimate the PSD of porous media by image analysis, which has a fast result and preserves the sample. The method requires the digital reconstruction of the porous medium by creating a stack of images that should be spaced by a length equal to the pixel size used on these images. To overcome this problem, Yang suggests to resize the image stack to match the image spacing to the pixel size, which reduces the image stack resolutions and increase the errors. To avoid the resizing procedure and its consequences, this paper tested three different approaches: the first one consisted in using the method proposed by Yang and collaborators without resizing the images; the second approach consisted in approximating the pores to spheres and analytically calculate their volumes; and the last approach was to approximate the pores to prolate spheroids and analytically calculate their volumes. The results showed that the first and second approaches were more efficient than the resizing alternative and that the third approach could be used to improve the results from the other two approaches.

Keywords: Pore-size distribution, Image spacing, Pixel size, no-resizing.

1 Introduction

The pore-size distribution (PSD) is an important property of porous media. It expresses how the pore volume in a porous medium is distributed in terms of pore size, i.e., how the total pore volume of a sample is distributed into pores having different sizes. Hence, the PSD identifies the relative of each pore size to the total pore volume, thus exposing which pore sizes are the most important of the sample, and which are the least important (having a small contribution to the overall pore volume). Fig. 1 shows an example of a pore-size distribution curve. PSD data have extensive application to various porous media problems in such diverse fields as the soil science, hydrogeology and petroleum, for example to quantify the water retention [1] and relatively permeability of soils or oil reservoir rocks [2].

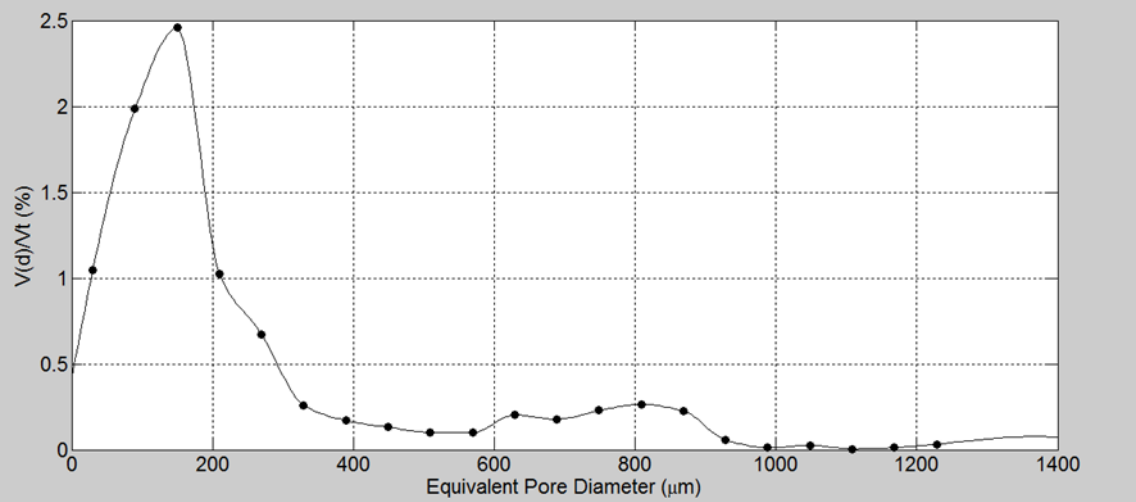

Figure 1. Pore-size distribution of a soil sample.

The importance of the PSD arises from its capability to characterizing a porous medium at its pore level. The problem of fluid flow in porous media is closely related to its microstructure in that such information as pore size, shape and connectivity has a crucial role in defining the underlying processes. Hence the PSD is often used to describe the porous microstructure since it provides direct information about the size of the pores and, indirectly, about related properties such as pore shape [3] and pore connectivity [4]. In addition, pore-size distribution information can be used to identify and predict various phenomena that may occur during contaminant transport. Predictions are then based upon the different effects on flow caused by pores of different sizes. According to Yang et al [5], larger pores have far more influence on the permeability by presenting less resistance to fluid flow, while finer pores have a major role in defining the capillary of a porous medium, the retention of wetting and non-wetting fluids, diffusion, and processes involving chemical reactions. Hence, by observing the pore-size distribution it is possible to identify which phenomena appear most relevant, and which likely are less important.

The PSD can be estimated using laboratorial tests that can last from days to weeks, depending upon the chosen method [6]. Many or most methods require the sample to be saturated with fluids that may have varying properties like wettability, while others expose the sample to high pressures, thus possibly affecting the mechanical stability of the sample (which is especially an issue for porous media composed of fragile or unconsolidated material). In order to provide an alternative method that could avoid some of these problems, Yang et al. [7] proposed an algorithm to estimate the PSD of a sample using image analysis. High resolution images are then obtained by means of X-ray microtomography, and used to identify the various pores and their sizes. The imaging process is done typically by evaluating multiple cross-sectional planes regularly spaced along the vertical direction (z axis) of a sample. For each plane to be evaluated, a two-dimensional image is created to represent the

corresponding cross-sectional plane (in the x and y directions). After all images are created, they are piled together into a stack, leading to a three-dimensional model of the sample. Once the process of imaging is done, the PSD is calculated numerically using an algorithm such as one developed by Yang et al. [7]. The results can be acquired quickly, depending on the size of the sample, the resolution of the image. and the hardware capability.

The method proposed by Yang and collaborators is a direct way to measure the pore-size distribution and does not require invasive practices, thus preserving the porous medium sample. But as an image-based algorithm, their method has the same disadvantages as commonly occurs with image techniques. Image-based processes are extremely dependent on the image resolution. In order to identify all of the pores present, or at least a representative part of them, the pixel size has to be in accordance to the pore sizes of the medium. In an image, each pixel represents an area where all of the information in the sample cannot be distinguished separately in that its value or color is a function of all the elements present. Hence, in order to properly identify the pores, the pixel size has to be small enough so that it can be filled completely or mostly by the pores. If the pixel size used in an acquired image is not well-suited for the porous medium, the image will not exhibit all pores and therefor become not representative. Thus, the pixel size of an image is a major factor to the success of any image-based process [8]. When an image has a small pixel size the image is said to have a high resolution, leading to a better definition and representation of the porous sample. Unfortunately, even high-resolution images often still have small pores that are not detectable. These pores are commonly referred to as sub-resolution pores. As long as they represent only a small fraction of the total porosity, they do not necessarily invalidate the usefulness of the images.

2 The Yang et al. algorithm

The algorithm proposed by Yang et al. [7] requires the images to be segmented only in two phases: a solid and a porous phase. This segmentation can be performed with Otsu's method [9], which uses a statistical analysis to define each pixel as being either a pore or a solid area. After segmentation, the images are binarized between the pore system and the solid matrix, which means that each pixel has either the value one (for pore areas) or zero (for solid areas).

Working with the binarized images, and assuming that the pores can be approximated as spheres, the proposed algorithm is run in four stages. The first stage is to analyze the pixels having a value of one (representing pores) so as to identify the biggest sphere that can be composed by connecting unity-valued pixels (this ensures that the considered sphere is contained in the pore region), with a particular analyzed pixel as its center . The radii of these spheres, referred to as critical radii, are measured by the number of pixels involved. Each pixel with a value of one may have its own critical radius.

The second stage is to identify which is the biggest critical radius of the sample, and to mark all pixels that compose the corresponding spheres as being part of a pore of that equivalent size. Once a pixel has been registered to a specific critical radius, it cannot be registered to another value. After all pixels composing the larger pores have been connected to the corresponding critical radius, the third stage is to repeat the previous step with the second biggest critical radius, then the third biggest critical radius, and so on until the smallest one. The fourth and last stage is to count how many pixels have been connected to each critical radius. By doing so, the incremental volume of each pore size can be estimated by calculating the volume of a voxel and multiplying by the number of voxels (equal to the number of pixels) of each pore size.

The algorithm was developed based on mercury intrusion porosimeter (MIP) methods, which estimate the pore-size distribution of a porous sample using a relation between the applied pressure and the pore radius being intruded. The MIP approach is performed using an apparatus that contains the sample and a certain volume of mercury. Starting with low values of the pressure, the methodology calculates the volume of mercury outside the sample and then increases the external pressure on the fluid by a small step. If the higher pressure is enough to overcome the capillary pressure on the external pores, mercury must flow inside the sample and fill the pores. When the volume of fluid

outside the sample is calculated again, the volume that flowed inside the pores can be estimated and related to the correspondent radii, which can be calculated in terms of the pressure using:

$$R = \frac{2\sigma}{P}. \quad (1)$$

in which R represents the pore radius, σ is the mercury-vacuum surface tension (assumed to be known), and P is the applied pressure, which is changed in small steps throughout the test. By using Eq. (1), the MIP method assumes that the mercury will intrude the sample starting with the largest pores and then penetrating into the smaller pores as the pressure increases. The largest pores hence are identified first and then the smaller ones. We followed the same sequence of identification of the pore sizes as used by Yang et al. [7].

3 The problem of the vertical resolution

The MIP method assumes that the pores all have a spherical shape in order to estimate their equivalent radius in terms of the pressure. The algorithm proposed by Yang and collaborators assumed a spherical shape of the pores as well, which implies some requirements of the acquired images. To be able to construct spheres, the voxels must have the same length in all directions (x, y and z). The voxel lengths are defined by the pixel size, with the pixel having the same length in both the x and y directions as standard. But the length of the voxels in the z direction is defined by the distance between two images. When this distance is larger than the pixel size, it is not possible to create spheres using the voxels since the distance from the center to the extremity must be the same in all directions. Instead, in these images the distance may then be larger in the z direction than in the other directions, which requires that, alternatively, prolate spheroids must be constructed rather than spheres.

While using stacks that have their z-spacing different from the pixel size is not ideal, sometimes it is still practical, especially when working with high-resolution images. Stacks for which the z-spacing is larger than the pixel size, require fewer cross-sectional planes to be analyzed, leading to fewer images and a much quicker imaging acquisition process. Another possible reason for not having the z-spacing equal to the pixel size is the technical limitation of the device used for the image acquisition. Some equipment cannot achieve the same resolution in the z-axial direction as used in the x and y directions.

Irrespective of the reasons of why the length between two images is larger than the length of a pixel, the resulting stack is not suitable for analysis using the algorithm of Yang and collaborators. For these situations, Yang et al. [7] recommend a precursor step in order to allow the stack to be analyzed using their algorithm. This initial step consists of resizing the image stack and changing the voxel lengths in the three directions in order to make them equal. But the process of resizing the images has some downsides, notably a loss of resolution and more uncertainty. During resizing, the stack loses some of the images, and with each image losing some pixels. The process blends pixels, which causes some loss of data and might lead to less accurate results.

To avoid these problems, this paper investigates an alternative way of estimating the pore-size distribution of image stacks that have a vertical resolution different from the horizontal resolution (the resolution of the two-dimensional images) without resizing the images but still using the algorithm of Yang et al [7].

4 Methodology and results

In this paper, three different approaches were tested to calculate the PSD of a non-equally sized stack (i.e., having a vertical resolution different from the image resolution). One approach is based on the assumption that small differences between the image distance and the pixel size are not enough to create a considerable error. In this case, the resultant prolate spheroid should be close to a sphere, with the stack becoming suitable for analysis with the algorithm of Yang and collaborators without

requiring image resizing. This assumption is based on the similarity to a sphere of by prolate spheroids whose biggest axis is just slightly larger than the other ones. Another reason to extend the algorithm also to prolate spheroids is that there is no need then to establish the exact shape of the pore (as being spherical or otherwise). In the MIP method, Eq. (1) is used based on several assumptions and simplifications to relate the pressure to a certain value of the radius, but in Yang et al.'s algorithm no relation exists between the pressure and the shape of the pore. This permits one to use the algorithm to explore other pore shapes as well.

The second approach tested in this paper was again based on the assumption that prolate spheroids can be approximated by spheres, but in this case the pore-volume is calculated in a different way as done by Yang et al. In this approach, the pore-volume is estimated using analytical calculations of the spherical volume of the critical radius (the procedure to identify the critical radius is the same as in the regular algorithm). After calculating the volume of a sphere of a certain critical radius, its volume is then divided by the number of voxels that compose the sphere, leading to a volume/voxel rate. By knowing how many voxels are related to each critical radius, a simple multiplication of the number of voxels by the volume/voxel rate would give the total volume of pores corresponding to a specific critical radius. It is important to emphasize that by doing this, the voxels represent a virtual volume (different from the volume originally represented in the image), with a different volume for each different critical radius. This may lead to an underestimation of the pore volume when compared to the volume originally represented by the unity-voxels in the image.

The third approach assumes that the pore volume cannot be approximated by spheres, but considers the prolate spheroids instead. In this approach, like in the second one, the critical radii are identified using the Yang et al.'s algorithm, while the volumes of the different spheroids are calculated analytically. The volume/voxel rate is then defined and multiplied by the number of voxels associated with each critical radius to give the pore volume of each identified pore size. The z-axial radius (the major radius of the spheroid) has now a specific relation with the minor radius that is uniform throughout the stack. This relation is defined by the vertical resolution. The z-axial radius is hence written in terms of the minor radius, which is designated to be the critical radius in the algorithm. Eq. (2) below shows how the radii relate to each other, with R_M being the major radius, R_V the vertical resolution factor and R_m the minor radius (i.e., critical radius in the algorithm). Eq. (3) further shows how the vertical resolution factor is calculated. In Eq. (3), R_V is the vertical resolution factor, Δz the distance between two images and P_S the pixel size.

$$R_M = R_V . R_m \tag{2}$$

$$R_V = \frac{\Delta z}{P_S} \tag{3}$$

As in the second approach, the voxels in this procedure represent a virtual volume (a volume fraction of a continuous prolate spheroid) and not the original one. This approach may lead to an overestimation of the pore volume as compared to the volumes originally represented by the unity-voxels in the image.

Tests of the three different approaches consisted of estimating the pore-size distribution of eight samples using each model and comparing results with those obtained using the algorithm of Yang *et al* [7]. The analyzed samples were from two different soils, whose image stacks were provided by Embrapa (São Carlos, SP) and other papers have already used these samples ([6], [10] and [11]). For each soil, four stacks having different image resolutions were constructed using pixel sizes of 30, 12, 6 and 3.6 µm, with z-spacings equal to the pixel size, what make the stacks suitable for the Yang *et al.* algorithm. It was necessary to use stacks suitable for their algorithm so that we could properly estimate the PSD of all samples and compare our results obtained with the three different models with their approach. In order to create stacks with z-spacings different from the pixel size (so we could use the models), we removed some images from the original stack, thus increasing the new z-spacing. In this way we created stacks describing the same samples, but with lower resolutions.

The procedure to build the new stacks was to keep alternately an image and remove the next one. At the end of the procedure, the new stacks hence had half the number of images as the original ones, but still with the same length in the vertical direction, thus implying that the distances between

two images in the new stacks were twice as large. Since the z-spacing of the original stacks was equal to the pixel size, the new stacks had z-spacing that were double of the pixel size.

After estimating the pore-size distributions of the samples using both the original stacks (by means of the algorithm of Yang *et al.*) and the derived stacks (using our three proposed methods mentioned before), the mean squared error (MSE) of each method was calculated. Table 1 shows the MSE values of each method for all samples.

Table 1. Method's squared errors for all samples

Sample	Resolution (μm)	Method 1	Method 2	Method 3
Sample 1	30	2.65×10^{-4}	2.10×10^{-4}	1.50×10^{-3}
Sample 2	12	5.98×10^{-4}	8.35×10^{-4}	1.60×10^{-3}
Sample 3	6	8.37×10^{-4}	1.30×10^{-3}	8.00×10^{-3}
Sample 4	3.6	4.42×10^{-4}	7.43×10^{-4}	4.80×10^{-3}
Sample 5	30	3.83×10^{-5}	6.27×10^{-5}	5.09×10^{-4}
Sample 6	12	7.97×10^{-5}	9.66×10^{-5}	8.83×10^{-4}
Sample 7	6	1.18×10^{-4}	1.86×10^{-4}	1.70×10^{-3}
Sample 8	3.6	5.13×10^{-5}	7.83×10^{-5}	6.29×10^{-4}

Table 1 shows that Method 1, which applied the same algorithm as used by Yang et al. to the non-suitable stacks, had the smallest errors. Method 2 (which approximated the prolate spheroids by spheres) was intermediate, and Method 3 (which considered the pore shape as prolate spheroids and calculated their volumes analytically) had the largest MSE values. These results show that the worst approximation of the results by Yang et al.'s was obtained using Method 3.

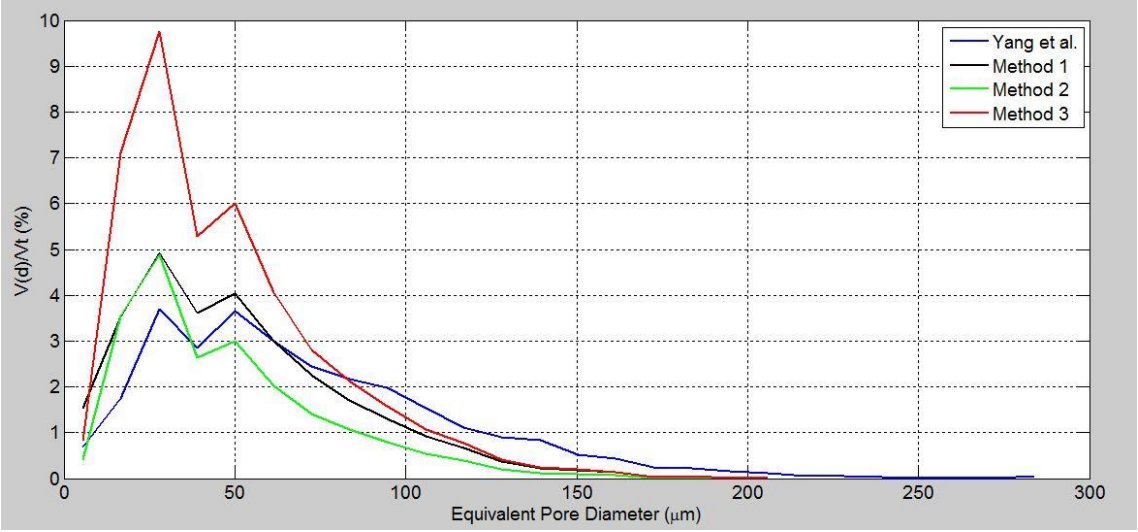

Figure 2. Pore-size distributions estimated using the three methods, and compared with results obtained using the algorithm of Yang et al. (in blue).

The blue curve in the figure represents the algorithm proposed by Yang et al [7]. As expected from Table 1, the figure shows that Method 1 produced results closest to the blue curve. Fig. 2 also shows that the curve generated with Method 1 was generally situated above the curve using Method 2, but below the Method 3 curve, thus reflecting under- and over-estimation of the PSD using these two methods, respectively.

Although Method 3 was the least representative, Fig. 2 shows that starting at an equivalent pore diameter of approximately 75 μm, Method 3 had the best results. The same behavior can be observed for the other samples as well, which can be explained by the characteristic overestimation of the methods. It shows that Method 3 results for this region can be used together with the results of Method 1 for the lower pore diameters (<75 μm), thereby creating an overall new curve with improved accuracy. A possible criterion to identify the region where Method 3 would give better results is to find the equivalent pore diameter (starting from the third one) where results obtained with methods 1 and 3 have a difference equal or less than 0.5%. This criterion satisfied all of our samples.

The derived stacks were resized next using the ImageJ – Fiji software. We opted to resize the images by doubling the new pixel size relative to the original size, thus making it the same as the z-spacing. By doing so, the resizing process did not need to reduce the number of slices (which would have added even more uncertainty to the process). Once all stacks were resized, the algorithm proposed by Yang et al. [7] was implemented and the results compared to those estimated using the original stacks. Table 2 shows the mean squared errors for the resized stacks compared to the original values, and also the mean squared errors for the non-resized stacks obtained using the combination of methods 1 and 3.

Table 2. Squared errors (MSE) for all samples with and without resizing

Sample	Resolution (μm)	Resizing	No resizing
Sample 1	30	9.47×10^{-5}	1.74×10^{-4}
Sample 2	12	9.15×10^{-4}	4.53×10^{-4}
Sample 3	6	2.00×10^{-3}	6.81×10^{-4}
Sample 4	3.6	1.50×10^{-3}	4.02×10^{-4}
Sample 5	30	5.23×10^{-5}	4.26×10^{-5}
Sample 6	12	3.51×10^{-5}	6.69×10^{-5}
Sample 7	6	1.15×10^{-4}	1.04×10^{-4}
Sample 8	3.6	5.13×10^{-4}	7.83×10^{-5}

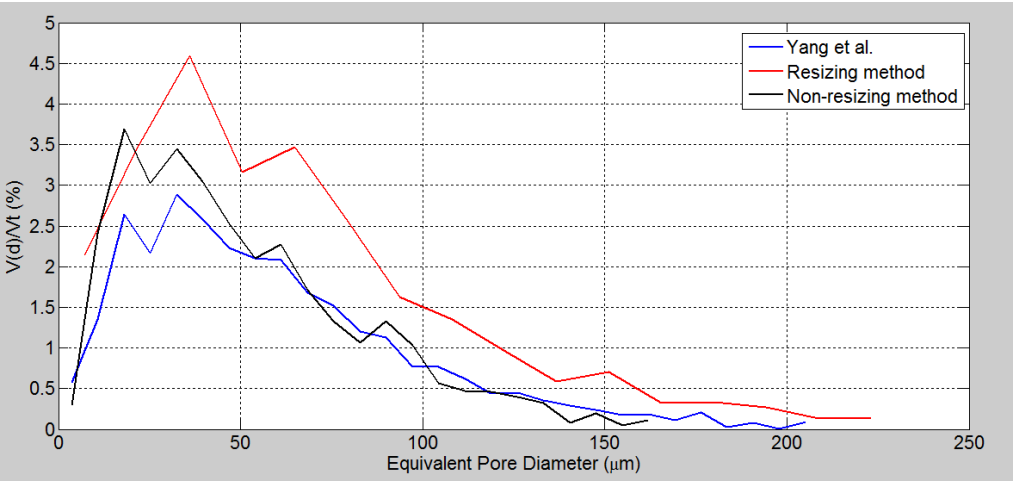

Figure 3. Pore-size distribution estimated by the resizing and no-resizing methods and compared to the result of Yang *et al.*'s algorithm in blue.

Figure 3 shows that there are differences between the maximum pore diameters identified by the proposed methods: while the blue PSD curve (estimated on the original and proper stack) has a maximum equivalent pore diameter around 205 μm, the black PSD curve (estimated by the no-resizing methods) has the shortest maximum equivalent pore diameter (around 162 μm) and the red PSD curve has the largest maximum equivalent pore diameter (around 220 μm). The difference between the maximum equivalent pore diameters of the blue and the black curve is a straight consequence of the number of pixels in the different stacks. The original stacks have double of the number of images present on the created stacks, so it favors the identification of larger pores. The created stacks, on the other hand, have fewer images then the original ones (half the number of images, so half the number of pixels), which hinders the identification of larger pores. So, for that reason, the no-resizing method has a shorter limit of analysis than the method performed on proper sized stacks and the resizing method. The reason for the larger maximum equivalent pore diameter on the red curve, however, is the use of greater pixels, which leads to a less accurate result. Figure 3 shows that both resizing and no-resizing methods were capable to reproduce (with different accuracies) the main peaks presented by the blue curve. However, the red curve has an offset to the right, representing the higher volume fractions on different pore diameters from that identified by the blue curve. This shift to the right means that the resizing method tends to overestimate the pore-sizes, thus the method fails to detect the smaller pores and reaches larger equivalent pore diameters that were not described on the original stacks. Table 3 shows the difference between the maximum equivalent pore diameters for all the samples.

Table 3. Maximum equivalent pore diameter for the different methods

Sample	Original Stacks (μm)	Created Stacks (μm)	Created and Resized Stacks (μm)
Sample 1	1228.06	868.63	1258.013
Sample 2	732.93	540.68	744.94
Sample 3	284.08	206.09	300.38
Sample 4	205.20	162.00	223.20
Sample 5	1108.25	808.722	1138.20
Sample 6	588.74	516.65	600.76
Sample 7	319.61	256.94	313.35
Sample 8	147.60	104.40	169.2

5 Summary and conclusions

Comparing the results obtained by analyzing resized images and the approaches presented in this paper we can affirm that two of the proposed methods had smaller errors. Calculating the mean from the squared errors for each sample, the resizing procedure had a mean equals to 6.73x10-4, while the first approach (applying the Yang et al.'s algorithm without resizing the images) had a mean equals to 3.39x10-4, the second approach (approximating the prolate spheroids to spheres and analytically calculating its volumes) had a mean equals to 4.90x10-4 and the third approach (analytically calculating the volume of the prolate spheroids) had a mean equals to 2.7x10-3. So, evaluating the errors produced by the presented approaches, we can conclude that the third one cannot be considered a good alternative, since the resizing method had a smaller error. On the other hand, it was also mentioned that part of the results given by the third approach could be used to improve the other methods. By combining the results from the first and third approach it was possible to achieve the smallest squared errors with a mean equals to 2.75x10-4.

Besides the difference of the squared errors, another advantage that was presented by the no-resizing methods was the greater accuracy on the equivalent pore diameter analysis. These methods were more successful to identify the pore diameters associated to the main peaks that the PSD curve from the original stacks presented. However, the no-resizing methods were not capable to identify the larger pores presented on the PSD curves from the properly spaced stack, having a shorter maximum

equivalent pore diameter.

Evaluating the presented differences on the identification of pore diameters responsible for the peaks of porous-volume fraction and considering that smaller errors denote better representations, we can conclude that the first and second approaches generated better results than the resizing method for the samples used in this paper. Applying the algorithm proposed by Yang et al. on the stacks that did not have the images spaced by the same length of the pixel size had better results than any other isolated methods. Also, by combining the Yang et al.'s algorithm to the third method the results were improved. Despite that, it is possible to see on Fig. 2 and Fig. 3 that even the best approximating methods had considerable deviation from the PSD curves estimated on the stacks with proper image spacing. That can be justified by the low vertical resolution caused by the large distance between the images. In this paper the z-spacing used was double of the pixel size, a critical value if compared to other stacks like the one mentioned by Yang et al. [7], where the z-spacing was equivalent to 1.075 of the pixel size. This high ratio between the z-spacing and the pixel size increases the inherent uncertainty of the image analysis processes, lowering the quality of the results. Another reason for the presented deviations is the fact that we are comparing results obtained by processes run on different resolutions. Since the created stacks had only half the data of the original ones (because it had only half of the total images) it is natural to have mismatches on the results.

Acknowledgements

This research was carried out in association with the ongoing R&D project registered as ANP nº 20163-2, "Análise Experimental da Recuperação de Petróleo para os Carbonatos do Pré-Sal do Brasil através de Injeção Alternada de CO2 e Água" (UFRJ/Shell Brasil/ANP), sponsored by Shell Brasil under the ANP R&D levy as "Compromisso de Investimentos com Pesquisa e Desenvolvimento". Also, this study was financed in part by the Coordenação de Aperfeiçoamento de Pessoal de Nível Superior- Brasil (CAPES) - Finance Code 001 and was developed upon the support received from CNPq "Conselho Nacional de Desenvolvimento Científico e Tecnológico - Brasil". We also would like to thank Dr. Carlos Vaz, from Embrapa/São Carlos, for providing the images from the soils and LRAP ("Laboratório de Recuperação Avançada de Petróleo") for the infrastructure.

References

[1] E. Q. Cunha; L. F. Stone; J. A. A. Moreira.; E. P. B. Ferreira; A. D. Didonet. Atributos físicos do solo sob diferentes preparos e coberturas influenciados pela distribuição de poros. Revista Brasileira de Engenharia Agrícola e Ambiental, vol. 14, n.11, pp. 1160 – 1169, 2010.

[2] N. T. Burdine. Relative permeability calculations from pore size distribution data. Petroleum Transactions of AIME, vol. 198, pp. 71 – 78, 1953.

[3] J. Schoelkopf; P. A. C. Gane; C. J. Ridgway; G. P. Matthews. Influence of inertia on liquid absorption into paper coating structures. Nordic Pulp & Paper Research Journal, vol. 15, pp. 422–430, 2000.

[4] T. M. Freyman; Yannas, I. V.; Gibson, L. J. Cellular materials as porous scaffolds for tissue engineering. Progress in Materials Science, vol. 46, pp. 273–282, 2001.

[5] Z. Yang; X. F. Peng; M. Y. Chen; D. J. Lee; J. Y. Lai. Intra-layer flow in fouling layer on membranes. Environmental Science & Technology, vol. 43, pp. 3248–3253, 2009.

[6] F. A. M. Cássaro; A. N. P. Durand; D. Gimenez; C. M.P. Vaz. Pore-size distributions of soils derived using a geometrical approach and multiple resolution microct images. Soil Science Society of America Journal, pp. 468-476, 2017.

[7] Z. Yang; X. F. Peng; M. Y. Chen; D. J. Lee. An image-based method for obtaining pore-size distribution of porous media. Environmental Science & Technology, vol. 43, pp. 3248–3253, 2009.

[8] T. Bultreys; W. Boever; V. Cnudde. Imaging and image-based fluid transport modeling at the pore scale in geological materials: a practical introduction to the current state-of-the-art. Earth-Science Reviews, vol. 155, pp. 93-128, 2016.

[9] N. Otsu. A threshold selection method from gray-level histogram. IEEE Trans. Syst. Man. Cybern., vol. 9, pp. 62–66, 1979.
[10] C. M. P. Vaz; I. C. Maria; P. O. Lasso; M. Tuller. Evaluation of an advanced benchtop micro-computed tomography system for quantifying porosities and pore-size distributions of two Brazilian oxisols. Soil Physics, vol. 75, n. 3, pp. 832 – 841, 2011.
[11] C. M. P. Vaz; M. Tuller; P. R. O. Lasso; S. Crestana. New perspectives for the application of high-resolution benchtop x-ray microCT for quantifying void, solid and liquid phases in soils. Soil Physics, pp. 261 – 281, 2014.